A guarded hot box procedure for determining the dynamic response of full-scale wall specimens - Part I

NRCC-34002

Brown, W.C.; Stephenson, D.G.

January 1993

A version of this document is published in / Une version de ce document se trouve dans:
ASHRAE Transactions, 99, (1), ASHRAE Winter Meeting, Chicago, IL, USA, January-23-93), pp. 632-642, 93 (Paper presented at the ASHRAE Winter Meeting held in Chicago, IL, USA, January 23-27, 1993)

A GUARDED HOT BOX PROCEDURE FOR DETERMINING THE DYNAMIC RESPONSE OF FULL-SCALE WALL SPECIMENS—PART I

W.C. Brown

D.G. Stephenson, Ph.D.

ABSTRACT

ASHRAE Research Project 515 had the goal of producing measured values of the dynamic heat transmission characteristics of walls. The characteristics were measured in a guarded hot box facility. The facility, which conforms in general to that standardized by ASTM C236, measures heat transfer through a 2440 mm × 2440 mm (8 ft × 8 ft) test area. Calorimeter temperatures are controllable between 16°C and 26°C (60°F and 80°F), and cold-side temperatures are controllable between 0°C and −40°C (32°F and −40°F). Data acquisition and control are provided through a laboratory computer system.

Dynamic calibration of the guarded hot box facility was required before it could be used to measure dynamic heat transmission characteristics. This calibration was developed from first principles and supported by measurements of a 102 mm (4 in.) thick expanded polystyrene specimen whose thermal characteristics had been determined from measurements of material properties. To measure the dynamic heat transmission characteristics of wall specimens, a test and data reduction procedure was also developed from first principles. The validity of this procedure was confirmed with measurements of the dynamic heat transmission characteristics of a 203 mm (8 in.) thick cement mortar specimen whose thermal characteristics were determined from measurements of material properties.

INTRODUCTION

The z-transfer function data and procedure published in the *1989 ASHRAE Handbook—Fundamentals* (ASHRAE 1989) are the basis of most methods for calculating dynamic heat transmission through walls. These data and procedures pertain to walls made up of layers of homogeneous materials and have no allowance for thermal bridges, such as framing members or brackets that support cladding. Hot box facilities as standardized by ASTM (1991a, 1991c) are limited to measuring the steady-state heat transmission characteristics, including R-value, of walls. However, recent work by Burch et al. (1987) and Stephenson et al. (1988) has proposed procedures to use these same facilities to measure the dynamic heat transmission characteristics of walls.

ASHRAE Technical Committee 4.1, Load Calculations, Data, and Procedures, initiated Research Project 515 to address the issue of measured versus calculated dynamic thermal performance characteristics. The project had two objectives:

1. to measure the dynamic heat transmission characteristics of seven generic types of walls in order to determine the coefficients of the two transfer functions that incorporate these characteristics, and
2. to confirm the testing and data reduction procedures used in RP-515 by using these procedures to measure the dynamic heat transmission characteristics of a homogeneous wall specimen of "known" characteristics.

The first objective was designed to determine whether the dynamic heat transmission characteristics of nonhomogeneous walls differ significantly from the response that would be predicted using *Fundamentals* (ASHRAE 1989) methods. It is documented in a companion paper (Brown and Stephenson 1993). The second objective, which was designed to demonstrate that the measurement procedure used with the seven generic walls produced accurate data, is documented in this paper. It presents a description of the guarded hot box facility and the dynamic calibration of the facility. It also confirms the validity of the testing and data reduction procedure for measuring dynamic heat transmission characteristics by demonstrating that the procedure can measure the characteristics of a homogeneous cement mortar test specimen. Both objectives are documented in the final contract report (Brown 1991).

GUARDED HOT BOX FACILITY

The guarded hot box facility (Figure 1) conforms, in

William C. Brown is a senior researcher at the Institute for Research in Construction, National Research Council Canada, Ottawa, Ontario. **Donald G. Stephenson** is a private consultant who was formerly with the Institute for Research in Construction.

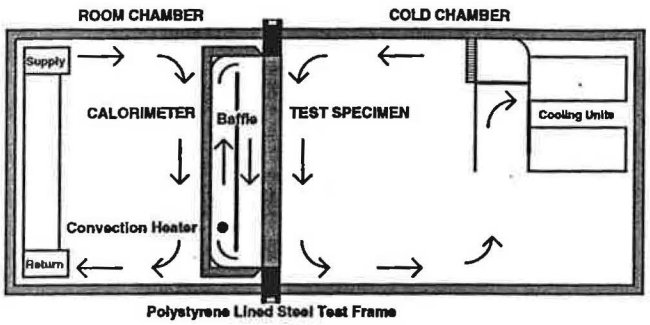

Figure 1 Section through guarded hot box facility.

general, to that standardized by ASTM C236 (1991a). It consists of a cold chamber with test temperatures between 0°C and −40°C (32°F and −40°F), a metering box or calorimeter with test temperatures between 16°C and 26°C (60°F and 80°F), and a room chamber that serves as the thermal guard for the calorimeter. The calorimeter, with a 2440 mm × 2440 mm (8 ft × 8 ft) test area, measures the heat flow through a test specimen of similar size. The test specimen is mounted in an extruded polystyrene lined steel test frame. In this arrangement, the polystyrene performs as the perimeter thermal guard for the test specimen.

The calorimeter is constructed of 76 mm (3 in.) thick isocyanurate foam board stock that was assembled without thermal bridges. It is finished with fiberglass and polyester resin for physical protection. An equal-area, 64-junction thermopile is built into the top, bottom, sides, and back of the calorimeter to sense the temperature difference across the walls of the calorimeter. A baffle of fiberglass-surfaced, isocyanurate foam, 40 mm thick by 2440 mm wide by 2015 mm high (1.5 in. × 96 in. × 79 in.), is centered vertically in the calorimeter and 230 mm (9 in.) from the back wall.

The calorimeter air temperature is sensed with an RTD and is maintained at setpoint through a three-mode analog millivolt controller. The controller regulates a DC power supply that feeds an electric convection heater located between the back wall and the baffle. The heaters are raised above the bottom of the baffle so that the baffle shields the test specimen from direct radiation from the heaters. Heated air flows up between the back of the calorimeter and the baffle, through the gap at the top, down the 405-mm (16-in.) space between the baffle and the test specimen, and back through the gap at the bottom.

The cold chamber is constructed of 102 mm (4 in.) thick, aluminum-skinned, polyurethane-filled panels. Air in the cold chamber is circulated by a fan so as to fall parallel to the cold face of the specimen. The temperature is sensed with an RTD and is maintained at setpoint through a three-mode analog millivolt controller that regulates high-voltage AC power to an electric heater. The air is precooled below setpoint by passing it over a cooling coil fed from a central chiller plant.

The room chamber is also constructed of 102 mm (4 in.) thick, aluminum-skinned, polyurethane-filled panels. The room air temperature can be controlled in one of two modes. For steady-state tests, the room chamber acts as a thermal guard for the calorimeter. The air temperature is controlled through a three-mode analog null voltage controller so that zero temperature difference is maintained across the walls of the calorimeter. This temperature difference is sensed by the equal-area thermopile that is built into the calorimeter walls. For dynamic tests, the temperature is controlled at a fixed value. The temperature is sensed with an RTD and is maintained at setpoint through a three-mode analog millivolt controller. For both steady-state and dynamic tests, the controllers regulate AC power to an electric heater that heats air that has been precooled below setpoint by passing over a process chilled-water cooling coil.

A computer-based data acquisition and control system provides remote setpoints for the controllers and data collection and processing services for the facility. Calorimeter heater power is measured by a precision current shunt and voltage divider with an accuracy of better than 1%. Test temperatures are sensed with 30-gauge copper-constantan thermocouples with an accuracy of ±0.1°C. All sensors are measured continuously, and space and time average data for sensors of interest are recorded every 15 minutes. Analysis of the test data occurs off-line on another computer.

Remote setpoints for the relevant temperature controllers are supplied by the laboratory computer for both steady-state and dynamic tests. The setpoint can be programmed to follow a constant, a ramp, or a sinusoidal waveform. The practical limits on the sinusoidal period are 3 to 48 hours. During dynamic testing, the computer updates the setpoint every minute, and the controller regulates the air temperature to match the new setpoint. The option to control calorimeter heater power rather than calorimeter temperature is also available. With this option, the heater power can be programmed to follow a constant, a ramp, or a sinusoidal waveform.

DYNAMIC RESPONSE OF THE GUARDED HOT BOX FACILITY

Dynamic calibration of the hot box facility requires that the response of the facility to dynamic excitation be determined. The heat transfer processes in the hot box facility can be represented by the thermal circuit illustrated in Figure 2.

Heat is transferred to the warm surface of the specimen from two different sources: by convection, through resistance R_c, from the air that circulates in the calorimeter (T_h) and by radiation, through resistance R_r, from the baffle (T_{B2}). Given the hot box thermal circuit, the baffle surface temperature, T_{B2}, will always be lower than the air temperature, T_h. It is necessary that a single equivalent environmental temperature be determined that would represent the combined driving potential from the calorimeter to the

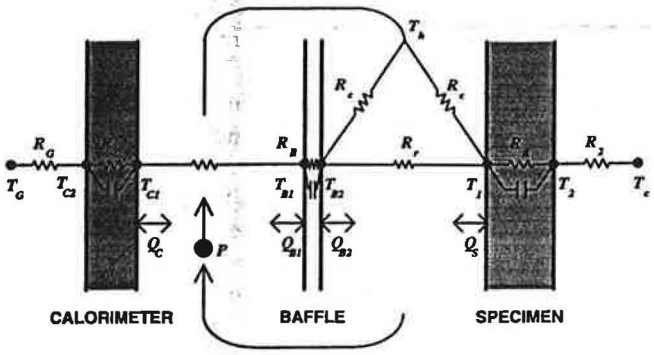

Figure 2 Guarded hot box facility thermal circuit.

specimen. The film resistance or heat transfer coefficient between the environmental temperature and the specimen must also be determined.

When the calorimeter and specimen are excited dynamically, heat is transferred into and out of the specimen, Q_S (see Figure 2). Heat is also transferred into and out of the inner surface of the calorimeter, Q_C, and both surfaces of the baffle in the center of the calorimeter, Q_{B1} and Q_{B2}. The calorimeter and baffle are each excited by measurable temperatures and have unique transfer functions relating the measured excitation temperatures to the heat transfer to/from the element. Determination of the dynamic response of the hot box facility, therefore, requires determination of the transfer functions for the calorimeter, C, and the baffle, B, that relate the heat transfer to/from the element to the temperatures on the surfaces of the element.

The transfer functions were determined using a 101-mm-thick expanded polystyrene test specimen. It was chosen because it was homogeneous, with a high R-value and a fast response, so that the response of the calorimeter would be the prominent response of the calorimeter/specimen system. The thermal characteristics of the specimen were determined by independent procedures. Thermal conductivity was determined from a series of heat flow meter tests (ASTM 1991b) at different mean temperatures; it was found to be well represented by a linear function of mean temperature. Volumetric heat capacity was determined by the method described by Stephenson (1987); it was also found to have a slight dependence on mean temperature.

Heat Transfer between Calorimeter and Test Specimen

As a first step in determining an equivalent environmental temperature, the delta resistance network, representing the heat transfer circuit between the air, the baffle, and the warm surface of the specimen, can be replaced by a star network (Figure 3). (Note that the delta circuit assumes that the convective heat transfer coefficient is the same at the face of the baffle and at the face of the specimen.)

In the star network, T_E is the equivalent environmental temperature and R_1 is the thermal resistance for combined

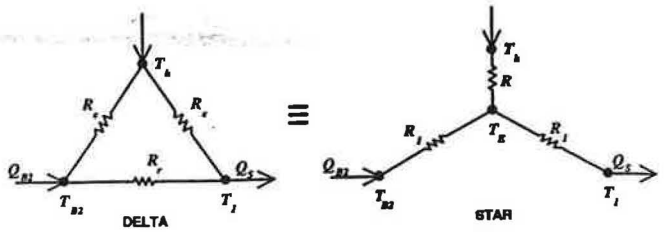

Figure 3 Delta to star substitution for calorimeter thermal circuit.

radiation and convection from T_E to the warm surface of the specimen at temperature T_1. Steady-state analysis of the revised thermal circuit for the hot box facility yields the following relationships:

$$R_1 = \frac{T_{B2} - T_1}{Q_S + Q_B} \tag{1}$$

$$T_E = T_{B2} - R_1 \cdot Q_B \tag{2}$$

$$Q_B = \frac{T_{B1} - T_{B2}}{R_B} \tag{3}$$

A series of steady-state tests on the expanded polystyrene calibration specimen were used to determine values of R_1. The test results and the values derived from them (Table 1) indicate that the value of R_1 is essentially independent of the heat flow through the specimen, Q_S, for heat flows between 50 W and 100 W. The mean value of 0.079 $m^2 \cdot K/W$ applies when the surface of the test specimen has an emissivity that is close to 1. If the surface of the specimen has a much lower emissivity, the value of R_1 would be somewhat larger. Equations 2 and 3 can be used to calculate an equivalent environmental temperature T_E for all tests, since R_1 and R_B are known and T_{B1} and T_{B2} can be measured.

Calorimeter Transfer Function, C

The cyclic component of the heat flows into the calorimeter walls, Q_{C1} and Q_{C2}, are related to the cyclic component of the temperatures at these surfaces, T_{C1} and T_{C2}, by

$$\begin{vmatrix} T_{C1} \\ Q_{C1}/A_C \end{vmatrix} = \begin{vmatrix} X_C & Y_C \\ Z_C & X_C \end{vmatrix} \bullet \begin{vmatrix} T_{C2} \\ Q_{C2}/A_C \end{vmatrix} \tag{4}$$

The square matrix is called the transmission matrix for the walls, and the matrix elements X_C, Y_C, and Z_C are functions of the thermal properties and dimensions of the materials in the walls and the frequency of the cyclic component (Carslaw and Jaeger 1959). A_C is the area of the calorimeter shell.

TABLE 1
Determination of R_1 from Steady-State Thermal Tests on the Expanded Polystyrene Calibration Specimen

Variable	Test A	Test B	Test C
T_c (°C)	-35.1	-20.4	-5.3
T_{B1} (°C)	20.9	21.0	21.1
T_{B2} (°C)	19.3	19.6	20.1
T_1 (°C)	17.9	18.6	19.4
T_2 (°C)	-34.1	-19.6	-4.9
Q_S (W)	100.6	76.1	49.7
T_m (°C)	-8.1	-0.5	7.2
R_1 (m²·K/W)	0.078	0.079	0.079
R_S (m²·K/W)	3.07	2.98	2.91
R_2 (m²·K/W)	0.060	0.060	0.048

The heat flow through the outside surface of the calorimeter, Q_{C2}, is related to the temperature in the room chamber or guard, T_G, and the outside surface, T_{C2}, by

$$Q_{C2} = \frac{T_{C2} - T_G}{R_G} \cdot A_C \tag{5}$$

Hence, when the temperature of the guard is kept constant, i.e., $T_G = 0$,

$$T_{C1} = (X + Y/R_G) \cdot T_{C2} \tag{6}$$

and

$$Q_{C1} = (Z + X/R_G) \cdot T_{C2} \cdot A_C \tag{7}$$

Combining Equation 6 with Equation 7 produces an expression relating the heat flow through the inner surface of the calorimeter, Q_C (= Q_{C1}), to the temperature difference across the calorimeter walls, ($T_{C1} - T_{C2}$):

$$Q_C = \left(\frac{Z_C + X_C/R_G}{X_C + Y_C/R_G - 1} \right) \cdot A_C \cdot (T_{C1} - T_{C2}) \tag{8}$$

The temperature difference across the calorimeter walls, ($T_{C1} - T_{C2}$), is related to the voltage from the thermopile across the calorimeter walls, E, and the sensitivity of the thermopile, k, by ($T_{C1} - T_{C2}$) = $k \cdot E$. Hence, the total heat flow into the inner surface of the calorimeter, Q_C, is

$$Q_C = \left(\frac{Z_C + X_C/R_G}{X_C + Y_C/R_G - 1} \right) \cdot A_C \cdot k \cdot E = C \cdot E \tag{9}$$

where

$$C = \left(\frac{Z_C + X_C/R_G}{X_C + Y_C/R_G - 1} \right) \cdot A_C \cdot k \tag{10}$$

Under steady-state conditions the heat flow through the calorimeter is

$$Q_{C1} = \frac{k \cdot E}{R_C} \cdot A_C \tag{11}$$

The value of $k \cdot A_C / R_C$ was determined to be 1.79 W/mV from a series of steady-state tests on the expanded polystyrene specimen. In these tests the temperatures inside the calorimeter and in the cold chamber were kept constant, and the temperature in the guard was held constant at several values above and below the calorimeter temperature. Thus the calorimeter transfer function C is

$$C = 1.79 \cdot R_C \cdot \left(\frac{Z_C + X_C/R_G}{X_C + Y_C/R_G - 1} \right) \tag{12}$$

Values of C have been calculated for various frequencies using the thermal properties and thickness of the calorimeter walls. These values are given in Table 2.

Baffle Transfer Function, B

The cyclic component of the heat flow into the surfaces of the baffle is related to the temperatures at the surfaces by

$$\begin{vmatrix} Q_{B1} \\ Q_{B2} \end{vmatrix} = \begin{vmatrix} X_B/Y_B & -1/Y_B \\ -1/Y_B & X_B/Y_B \end{vmatrix} \bullet \begin{vmatrix} T_{B1} \\ T_{B2} \end{vmatrix} \bullet A_B \tag{13}$$

where X_B and Y_B are elements of the transmission matrix for the baffle.

Thus the total heat flow into the baffle

$$\begin{aligned} Q_B &= Q_{B1} + Q_{B2} \\ &= \left(\frac{X_B - 1}{Y_B} \right) \cdot (T_{B1} + T_{B2}) \cdot A_B \\ &= B \cdot (T_{B1} + T_{B2}) \end{aligned} \tag{14}$$

TABLE 2
Values of the Calorimeter Transfer Function C for Various Frequencies

P (h)	ω (rad/s)	C (W/mV)
48	3.64×10^{-5}	2.145∠-327.0°
24	7.27×10^{-5}	2.962∠-308.0°
12	1.45×10^{-4}	5.033∠-292.4°
6	2.91×10^{-4}	9.460∠-283.9°
3	5.82×10^{-4}	17.998∠-280.4°

where

$$B = \left(\frac{X_B - 1}{Y_B} \right) \cdot A_B \qquad (15)$$

Values of B have been calculated for various frequencies using the thermal properties and dimensions of the baffle. These values are given in Table 3.

Confirmation of the Transfer Functions

The values of C and B given in Tables 2 and 3 have been confirmed by a series of dynamic tests with the 101-mm-thick polystyrene calibration specimen. The power input to the calorimeter, P, and the temperature of the room chamber, T_G, were kept constant, while the temperature in the cold chamber, T_c, varied sinusoidally. Tests were run for periods of 24, 12, 6, and 3 hours. The variation in cold chamber temperature produced a cyclic component of heat flow into the warm surface of the specimen, Q_S, which, in turn, generated a cyclic variation in heat flow into the calorimeter, Q_C, and into the baffle, Q_B. However, the net heat balance of the calorimeter is zero, i.e., $Q_B + Q_C = -Q_S$.

Measured surface temperatures of the specimen from the tests were used together with the independently determined thermal properties to calculate the cyclic component of heat flow into the warm surface of the specimen, Q_S, during the tests. As the thermal properties were functions of mean temperature, Q_S had to be calculated by a numerical method that allowed for the effect of the temperature dependence of the properties. The basis for this method is given in Appendix A.

The fundamental components of the Fourier series that were derived from the temperatures recorded during the steady periodic portion of each test were used with B and C to calculate Q_B and Q_C. Values of the sum of the cyclic components of Q_B and Q_C are given in Table 4 along with the cyclic component of Q_S derived from the surface temperatures and thermal properties of the test specimen. The close agreement between the predicted and measured values confirms that the values of B and C yield accurate values for the heat flow to/from the baffle and the calorimeter during dynamic testing.

TABLE 3
Values of the Baffle Transfer Function B for Various Frequencies

P (h)	ω (rad/s)	B (W/°C)
48	3.64×10^{-5}	0.966∠-270.1°
24	7.27×10^{-5}	1.931∠-270.2°
12	1.45×10^{-4}	3.862∠-270.4°
6	2.91×10^{-4}	7.718∠-270.7°
3	5.82×10^{-4}	15.391∠-271.4°

DETERMINING DYNAMIC HEAT TRANSMISSION CHARACTERISTICS

The z-transfer function data and procedure published in *Fundamentals* (ASHRAE 1989) only include z-transfer function coefficients that relate the heat flux component through the interior surface of the wall to the sol-air temperature on the exterior. This is sufficient to calculate the rate of heat transfer at the interior due to a change in exterior conditions, but another set of coefficients is needed when calculating the component of heat transfer at the interior due to a change in interior temperature. The latter is required for the calculation of room thermal response. Test and data reduction procedures for obtaining both sets of z-transfer function coefficients for a wall specimen were developed in support of RP-515. These procedures were presented in the final contract report (Brown 1991) and are reproduced in Appendix B.

Homogeneous Specimen

A 2440 mm × 2440 mm × 208 mm thick (8 ft × 8 ft × 8 in.) sand-cement mortar slab was cast as the "homogeneous wall specimen" to meet the second objective of the project. The slab contained no aggregate or reinforcing steel. Four 610 mm × 610 mm × 51 mm thick (24 in. × 24 in. × 2 in.) material test specimens were cast at the same time from the same material. These specimens were used to measure the thermal properties of the wall specimen. The wall and material specimens were left to cure in the laboratory for two months prior to testing.

Material Properties

The density, thermal conductivity, thermal diffusivity, and specific heat of the material test specimens were measured in our material test laboratory. These data are listed in Table 5. All data agree closely with *Fundamentals* values for this material. Density was determined from the dimensions of the test specimens and from their mass. The latter was measured with a precision balance having a

TABLE 4
Comparison of Predicted and Measured Values of Heat Flow into the Warm Surface of the Expanded Polystyrene Test Specimen (Referenced to T_c)

Period (h)	Q_B+Q_C (W/°C)	Q_S (W/°C)	| Diff | (W/°C)
48	---	---	
24	1.47∠ 1°	1.48∠ 0°	0.03
12	1.52∠ -8°	1.54∠-10°	0.06
6	1.53∠-22°	1.50∠-25°	0.10
3	1.39∠-45°	1.34∠-52°	0.16

TABLE 5
Physical Properties Determined for the Cement Mortar Homogeneous Test Specimen

	λ	ρ	C_p
mm [in.]	W/(m·K) [Btu/(h·ft²·F)]	kg/m³ [lb/ft³]	kJ/(kg·K) [Btu/(lb·F)]
208 [8]	1.71 [0.99]	2210 [138]	0.98 [0.23]

resolution of 1 g (0.0022 lb).

Two material test specimens with similar density and thickness were selected for thermal properties measurements. Four copper-constantan thermocouples were potted with epoxy flush with the face of each specimen. The specimens were then mounted together between the plates of an ASTM C-518 heat flowmeter apparatus (ASTM 1991b). This apparatus consists of two liquid bath temperature-controlled plates to which calibrated heat flux transducers are mounted. Heat flux through the combined material specimens was measured at two temperature conditions. The first was with an average temperature of about 23°C (74°F) and the second was with an average temperature of about 3°C (37°F). The temperature difference across each specimen was measured with the thermocouples embedded in each face. Thermal conductivity for each specimen was calculated from the respective temperature difference and thickness and the overall heat flux. The measured values of thermal conductivity did not vary with mean temperature.

The specific heat of the material specimens was determined from the thermal diffusivity of the specimens, which was, in turn, determined using a procedure developed by Stephenson (1987). For this procedure, a single bath was used to control the temperature of both plates; the test specimen/heat flow meter apparatus configuration was undisturbed. Thermal diffusivity was determined from measurements of the response of the paired specimens to a temperature ramp of approximately −4.7°C/h (−8.5°F/h) from an initial steady temperature condition at 35°C (95°F).

Test Results

Steps 3 and 4 of the test procedure (see Appendix B), which would normally have been conducted at an exterior temperature of −35°C (−31°F), were conducted at an exterior temperature of −20°C (−4°F), i.e., the same as that of steps 1 and 2. This was required because, given the low thermal resistance of the specimen, the heat flux at −35°C (−31°F) would have been beyond the capacity of the guarded hot box apparatus.

The steady-state and dynamic responses determined for the specimen are presented in Figure 4. The thermal resistance, R_S, determined at T_m = 24°C (75°F) was 97% of that predicted from the material thermal conductivity and the thickness of the specimen. The frequency response was measured at periods of 48, 24, 12 and 6 hours, and the values of $1/B$ and D/B were determined from these measurements. The response calculated from the b_n and d_n coefficients compares very well with that measured for the specimen and with that predicted from the material specimen properties. The c_n coefficients were determined from a fit to the data measured at the 12-hour period. The D/B response of the homogeneous specimen compared reasonably well with that predicted from the material specimen properties.

CONCLUSIONS

ASHRAE Research Project 515 had as a goal the measurement of the dynamic heat transmission characteristics of walls. While ASTM standardizes the guarded hot box as a method for measuring the steady-state heat transmission characteristics of walls, there is no standardized method of measuring the dynamic heat transmission characteristics of walls. An analysis of the guarded hot box facility used for this project provided a theoretical basis for determining the dynamic response of the facility. Measurement of the dynamic response of a 101-mm-thick polystyrene specimen and a 208-mm (8-in.) homogeneous cement mortar slab demonstrated that the guarded hot box can be used to determine the frequency response of full-scale wall specimens.

The series of tests on the cement mortar specimen demonstrated that the test and data analysis procedures used in ASHRAE Research Project 515 are capable of determining b_n and d_n coefficients that reproduce the $1/B$ frequency response very well and c_n (and d_n) coefficients that reproduce the D/B frequency response reasonably well. These results serve to validate the accuracy of the coefficients determined for the seven generic wall specimens (Brown and Stephenson 1993).

ACKNOWLEDGMENTS

John Richardson was responsible for the construction, instrumentation, and testing of the calibration specimens. Dr. Kunze Ouyang, China Academy of Building Research, People's Republic of China, provided many of the original ideas for the testing and analysis procedure and contributed immeasurably to their development.

REFERENCES

ASHRAE. 1989. *1989 ASHRAE handbook—Fundamentals.* Atlanta: American Society of Heating, Refrigerating and Air-Conditioning Engineers, Inc.

ASTM. 1991a. C 236-89: Standard test method for steady-state thermal performance of building assemblies by means of a guarded hot box. *Annual Book of ASTM Standards*, Vol. 04.06. Philadelphia: American Society for Testing and Materials.

Steady State Response

		Measured	Calculated	Predicted
T_m	°C [°F]	0 [32]	24 [75]	24 [75]
R_1	m²K/W [h·ft²·F/Btu]	0.078 [0.44]		
R_S	m²K/W [h·ft²·F/Btu]	0.12 [0.66]	0.12 [0.66]	0.12 [0.69]
R_2	m²K/W [h·ft²·F/Btu]	0.055 [0.31]		

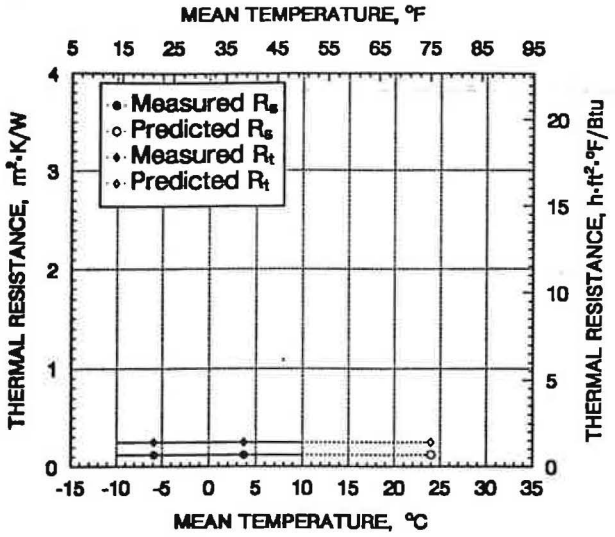

1/B Response

Period h	Measured Amp∠Phase	Calculated Amp∠Phase
48	0.84∠ -48°	0.81∠ -48°
24	0.58∠ -79°	0.57∠ -80°
12	0.32∠-119°	0.30∠-121°
6	0.13∠-172°	0.12∠-174°

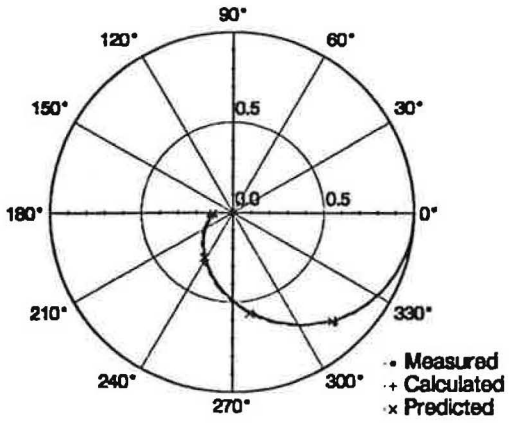

D/B Response

Period (h)	Measured Amp∠Phase	Calculated Amp∠Phase
48	1.65∠23°	1.53∠24°
24	2.06∠21°	1.94∠21°
12	2.44∠16°	2.23∠15°
6	2.77∠10°	2.44∠12°

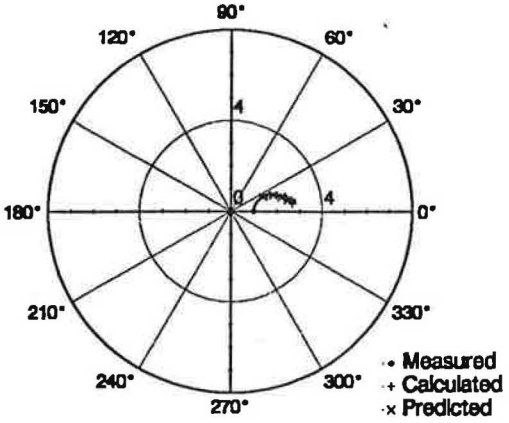

Figure 4 *Steady-state and dynamic response of cement mortar homogeneous test specimen.*

ASTM. 1991b. C 518-85: Standard test method for steady-state heat flux measurements and thermal transmission properties by means of the heat flow meter apparatus. *Annual Book of ASTM Standards*, Vol. 04.06. Philadelphia: American Society for Testing and Materials.

ASTM. 1991c. C 976-90: Standard test method for thermal performance of building assemblies by means of a calibrated hot box. *Annual Book of ASTM Standards*, Vol. 04.06. Philadelphia: American Society for Testing and Materials.

Brown, W.C. 1991. Final Report—ASHRAE Research Project 515-RP: Dynamic heat transmission characteristics of seven generic wall types and dynamic heat transmission characteristics of a homogeneous wall specimen. Ottawa, ON: National Research Council Canada.

Brown, W.C., and D.G. Stephenson. 1993. Guarded hot box measurements of the dynamic heat transmission characteristics of seven wall specimens, part II. *ASHRAE Transactions* 99(2).

Burch, D.M., R.R. Zarr, and B.A. Licitra. 1987. A dynamic test method for determining transfer function coefficients for a wall specimen using a calibrated hot box. *ASTM Symposium on Insulation Materials, Testing and Applications*, Bal Harbour, FL, December 6-9. ASTM Special Technical Publication 1030.

Carslaw, H.S., and J.C. Jaeger. 1959. *Conduction of heat in solids*, 2d ed. London: Oxford University Press.

Stephenson, D.G. 1987. A procedure for determining the thermal diffusivity of materials. *Journal of Thermal Insulation*, Vol. 10, April, pp. 236-242. Reprinted as NRCC 28337. Ottawa, ON: National Research Council Canada.

Stephenson, D.G., K. Ouyang, and W.C. Brown. 1988. A procedure for deriving thermal transfer functions for walls from hot-box test results. Internal Report No. 568. Ottawa, ON: National Research Council Canada.

APPENDIX A

Numerical Algorithm for Calculating Heat Flux into a Homogeneous Slab

The temperature distribution through a slab of homogeneous material, whose thermal conductivity and heat capacity are functions of the temperature, satisfies the differential equation

$$\rho C\left(\frac{dT}{dt}\right)=\lambda\frac{\partial^2 T}{\partial x^2}+\left(\frac{\partial\lambda}{\partial T}\right)\left(\frac{\partial T}{\partial x}\right)^2 \qquad \text{(A1)}$$

and the heat flux is

$$q=-\lambda\left(\frac{\partial T}{\partial X}\right) \qquad \text{(A2)}$$

As this equation is not linear when λ is a function of T, it is difficult to solve analytically and a numerical procedure was used. The calculation can be simplified by using the potential function

$$\eta=\int_0^T \lambda\cdot dT \qquad \text{(A3)}$$

This leads to

$$\frac{d\eta}{dt}=\frac{\lambda}{\rho C}\cdot\frac{d^2\eta}{dx^2} \qquad \text{(A4)}$$

and

$$q=-\frac{d\eta}{dx} \qquad \text{(A5)}$$

The thermal conductivity of polystyrene can be represented by a linear function of temperature,

$$\lambda=a+bT \qquad \text{(A6)}$$

$$\therefore \quad \eta=aT+bT^2/2 \qquad \text{(A7)}$$

and

$$T=\frac{-a+\sqrt{a^2+2b\eta}}{b} \qquad \text{(A8)}$$

Values of η are calculated iteratively at a set of equally spaced values of x and t using the usual finite difference approximations for the derivatives and values of λ and ρC that correspond to the value of T at each x and t.

$$\left(\frac{d\eta}{dt}\right)_t\cong\frac{3\eta_t-4\eta_{t-\delta}+\eta_{t-2\delta}}{2\delta} \qquad \text{(A9)}$$

$$\left(\frac{d^2\eta}{dx^2}\right)\cong\frac{\eta_{x+\Delta}-2\eta_x+\eta_{x-\Delta}}{\Delta^2} \qquad \text{(A10)}$$

where δ and Δ are the increments in the time and space coordinates respectively.

A good approximation for $-(d\eta/dx)_{x=0}$ (i.e., for $q_{x=0}$) can be derived from the Maclaurin series expansion about η_0:

$$\eta_\Delta=\eta_0+\Delta\left(\frac{d\eta}{dx}\right)_0+\frac{\Delta^2}{2!}\left(\frac{d^2\eta}{dx^2}\right)_0+\frac{\Delta^3}{3!}\left(\frac{d^3\eta}{dx^3}\right)_0+\cdots \qquad \text{(A11)}$$

$$\eta_{2\Delta}=\eta_0+2\Delta\left(\frac{d\eta}{dx}\right)_0+\frac{4\Delta^2}{2!}\left(\frac{d^2\eta}{dx^2}\right)_0+\frac{8\Delta^3}{3!}\left(\frac{d^3\eta}{dx^3}\right)_0+\cdots \qquad \text{(A12)}$$

The usual practice is to combine these two equations so as to eliminate the $(d^2\eta/dx^2)_0$ term and then neglect the $(d^3\eta/dx^3)_0$ and all higher order derivatives.

It is better, however, to combine them so as to eliminate the $(d^3\eta/dx^3)_0$ term and retain the $(d^2\eta/dx^2)_0$ term, which can be replaced by $(d\eta/dt)_0$ by using Equation A4. This means that the first neglected term is the fourth derivative rather than the third, and, consequently, this approximation for the $(d\eta/dx)_0$ has the

same order of accuracy as the approximation that is used for $d^2\eta/dx^2$ at the positions within the material:

$$q_{0,t} = \frac{7\eta_{0,t} - 8\eta_{\Delta,t} + \eta_{2\Delta,t}}{6\Delta} + \frac{\Delta}{3}\left(\frac{\rho C}{\lambda}\right)\left(\frac{d\eta}{dt}\right)_{0,t} - \frac{\Delta^3}{18}\frac{d^4\eta}{dx^4} \tag{A13}$$

Using Equation A8 to approximate $(d\eta/dx)_{0,t}$ and neglecting the fourth and all higher space derivatives gives

$$q_{0,t} \cong \frac{7\eta_{0,t} - 8\eta_{\Delta,t} + \eta_{2\Delta,t} + \left(\frac{\Delta^2}{\delta}\frac{\rho C}{\lambda}\right)_{0,t}\left(3\eta_{0,t} - 4\eta_{0,t-\delta} + \eta_{0,t-2\delta}\right)}{6\Delta} \tag{A14}$$

This approximation has been found to yield accurate values when δ is about 1% of the period of the highest frequency component of η_0, and when the Fourier number, $(\Delta^2/\delta)(\rho C/\lambda)$, is not more than about 1. The test for this accuracy is to repeat calculations with progressively smaller values of δ and Δ until there is no significant change in the values of $q_{0,t}$ from one calculation to the next.

APPENDIX B

Procedure to Measure Dynamic Heat Transfer Characteristics of Full Scale Specimens (from Brown 1991)

THEORY

The Laplace transforms of the interior temperature, T_i, and exterior temperature, T_e, for a wall are Θ_i and Θ_e, respectively, and the transforms of the heat fluxes through the wall surfaces, Q_i and Q_e, are Φ_i and Φ_e respectively. These can be related (Carslaw and Jaeger 1959) by a matrix expression, namely,

$$\begin{vmatrix}\Theta_i \\ \Phi_i\end{vmatrix} = \begin{vmatrix}A & B \\ C & D\end{vmatrix} \bullet \begin{vmatrix}\Theta_e \\ \Phi_e\end{vmatrix} \tag{B1}$$

The square matrix is called the transmission matrix of the wall. Matrix elements A, B, C, and D are functions of the thermal properties and dimensions of the materials in the wall and the surface heat transfer coefficients. Equation B1 can be recast as

$$\begin{vmatrix}\Phi_i \\ \Phi_e\end{vmatrix} = \begin{vmatrix}D/B & -1/B \\ 1/B & -A/B\end{vmatrix} \bullet \begin{vmatrix}\Theta_i \\ \Theta_e\end{vmatrix} \tag{B2}$$

The element C has been eliminated by using the fact that $AD-BC=1$. The functions D/B, $1/B$ and A/B are referred to as the Laplace transfer functions of the wall.

The transfer function $1/B$ can be represented as

$$1/B = \frac{U}{\prod_{n=1}^{\infty}(1+\tau_n s)} \tag{B3}$$

where

U = the thermal transmittance of the wall;
τ_n = the time constants of the wall, i.e., the poles of $1/B$ are at $s=-1/\tau_n$;
s = the Laplace transform variable.

Note that all of the transfer functions of Equation B2 have their poles at $s=-1/\tau_n$, since B is the common denominator.

When predicting the response of a wall or roof to environmental temperature variations, it is more convenient to use z-transforms of the temperatures and fluxes rather than the Laplace transforms. (The z-transforms are sometimes referred to as the time-series representations of these quantities.) An equation similar to Equation B2 relates the z-transform of interior heat flux, $Z\{Q_i\}$, to the z-transforms of temperature, $Z\{T_i\}$ and $Z\{T_e\}$, as follows:

$$Z\{Q_i\} = \frac{D(z)}{B(z)} \cdot Z\{T_i\} - \frac{1}{B(z)} \cdot Z\{T_e\} \tag{B4}$$

The poles of $D(z)/B(z)$ and $1/B(z)$ are identical because they have the same denominator and are the same as the poles of $1/B$. Thus, determination of the frequency response of the specimen permits determination of the principal poles of $D(z)/B(z)$ and $1/B(z)$.

The z-transfer functions can be expressed by

$$\frac{D\{z\}}{B\{z\}} = U \cdot \frac{\sum_{n=0}^{N_c} c_n \cdot z^{-n}}{\sum_{n=0}^{N_d} d_n \cdot z^{-n}} \tag{B5}$$

$$\frac{1}{B\{z\}} = U \cdot \frac{\sum_{n=0}^{N_b} b_n \cdot z^{-n}}{\sum_{n=0}^{N_d} d_n \cdot z^{-n}} \tag{B6}$$

where

z = $e^{s\Delta}$;
Δ = interval between successive terms in the time series for temperature and heat flux
N_c, N_b, N_d = the number of terms in the various sums
c_n, b_n, d_n = z-transfer function coefficients.

The d_n coefficients can be determined from the poles of $1/B$. The c_n and b_n coefficients can then be determined by matching the calculated response to the measured response.

Equation B4 can be written in the time domain as

$$d_0 \cdot Q_{i,t} = U \cdot \sum_{n=0}^{N_c}\left(c_n \cdot T_{i,t-n\Delta}\right) - U \cdot \sum_{n=0}^{N_b}\left(b_n \cdot T_{e,t-n\Delta}\right) - \sum_{n=1}^{N_d}\left(d_n \cdot Q_{i,t-n\Delta}\right) \tag{B7}$$

where

$Q_{i,t}$ = interior heat flow per unit area at time t
$T_{i,t}$ = interior environmental temperature at time t
$T_{e,t}$ = exterior environmental temperature at time t.

This form of the equation is equivalent to Equation 33 in Chapter 26 of *Fundamentals* (ASHRAE 1989). One significant difference between the two equations is that this form does not assume that the interior environmental temperature, $T_{i,t}$, is constant. Hence, with this equation, it is necessary to know the individual c_n coefficients rather than just the sum, as is required with the *Fundamentals* version. A second minor difference is that *U*-value is incorporated in the values of b_n and c_n tabulated in *Fundamentals*; it is not incorporated in the b_n and c_n coefficients of Equation B7.

Values of *D/B* for a test specimen can be determined by measuring the heat flux through the room side (interior) of the specimen in response to an excitation on the room side of the specimen. Similarly, values of *1/B* can be determined for a test specimen by measuring the heat flux through the room side of the specimen in response to an excitation on the outside (exterior) of the specimen. It should be noted that different values of *D/B* and *1/B* will be determined depending on whether the surface to surface or environment-to-environment response is measured, i.e., whether the interior and exterior film coefficients are included or not. The z-transfer function coefficients values listed in *Fundamentals* include fixed interior and exterior film coefficients.

A finite number of time constants can be determined from the experimental results that best match the response calculated with Equation B3 to the measured values of *1/B*. This finite series of time constants approximates the infinite series of time constants that theoretically represent the response of the specimen. Values of d_n for a given time interval, Δ, can then be determined by equating the denominators of *1/B(z)* (Equation B6) and *1/B* (Equation B3). The number of significant d_n coefficients determined by this procedure is dependent on the magnitudes of the time constants. These d_n coefficients are applicable to both *D(z)/B(z)* (Equation B5) and *1/B(z)* (Equation B6), and these equations can be used to determine values of b_n and c_n appropriate to the specimen under consideration.

A final point to be noted in a discussion of dynamic thermal performance is that the steady-state thermal properties of materials are, to a greater or lesser extent, a function of the mean temperature of the material. One consequence of this sensitivity is that the dynamic response will be sensitive to mean temperature. Thermal resistance of most insulation materials is especially dependent on the mean temperature of the material. The sensitivity of the thermal resistance of an insulated wall to mean temperature will depend not only on how sensitive the insulation is to mean temperature but also on the ratio of heat flux through the insulation to heat flux through the thermal bridge. The latter point is important because the thermal resistance of thermal bridges is not usually a function of mean temperature.

TEST PROCEDURE

The test procedure for measuring the dynamic heat transfer characteristics of full-scale wall specimens was executed in a guarded hot box facility that had been calibrated using the procedure described in the body of this paper. The procedure consisted of a series of measurements of the response of the test specimen, and facility, to sinusoidal variations of exterior temperature and of interior power. The steps in the procedure, which were all conducted with a mean interior temperature of approximately 21°C [70°F], are as follows:

1. Measure thermal resistance of the specimen with exterior temperature of -20°C [-4°F].
2. With guarded hot box calorimeter (interior) power fixed at that determined in Step 1 and mean exterior temperature fixed at -20°C [-4°F], measure response of the specimen to sinusoidal variations in exterior temperature of amplitude 15K [27°F] at periods of 24, 12, and 6 hours, plus 48 hours for heavier specimens.
3. Measure thermal resistance of the specimen with exterior temperature of -35°C [-31°F].
4. With mean calorimeter power fixed at that determined in Step 3 and exterior temperature fixed at -35°C [-31°F], measure response of the specimen to sinusoidal variations in calorimeter power of amplitude 60 W at periods of 24, 12, and 6 hours, plus 48 hours for the heavier specimens.
5. Thermal resistance was monitored throughout the test procedure by determining it from the mean values of temperature and heat flux that were measured for each test period in Steps 2 and 4 and also by repeating Step 1 at the end of the procedure. This latter test was conducted to ensure that no significant change had occurred to the specimen during the test series.

For the purposes of this research project, thermal resistance was also measured at an exterior temperature of -5°C [23°F]. This measurement provided a measured thermal resistance value at a third mean temperature and was used, with the values measured in Steps 1 and 3, to determined the mean temperature dependency of the thermal resistance.

Values of *D/B* for the specimen were determined at the test periods from the data measured in Step 4 and from the test apparatus dynamic calibration. Values of *1/B* for the specimen were determined at the test periods from the data measured in Step 2, from the test apparatus dynamic calibration, and from the values of *D/B* determined above. Data for both transfer functions were normalized to the thermal resistance measured for the specimen. Thus

variations in thermal resistance due to mean temperature were accommodated in the normalized transfer functions.

A minimization procedure was used to determine time constants that best matched the response calculated with Equation B3 to the measured values of $1/B$. Values of d_n were then determined by equating the denominator of $1/B(z)$ (Equation B6) with a time interval, Δ, of 1 hour to the denominator of $1/B$ (Equation B3).

Values of b_n were determined in three steps:

1. Equation B3 was used to calculate the response at 1 hour time intervals to a unit ramp temperature change.
2. The response to a unit triangular pulse was determined from the calculated ramp response; note that this produced the response factors for the specimen.
3. Equation B6 was used to generate b_n coefficients that matched the unit triangular pulse response.

Values of c_n were determined for most specimens by fitting Equation B5 to the frequency response measured at two periods, typically 24 and 6 hour. This gave an exact fit to the data at the fitted periods and produced a series of five coefficients that gave a good fit to the frequency response measured at 12 hour, and to 48 hour if it had also been measured. However, for the lighter specimens, a fit at only 12 hour gave a series of three coefficients that adequately represented the measured frequency response.